

Variability of measured railway track conductance due to test setup

Jacopo Bongiorno¹, Andrea Mariscotti²

¹ Università di Genova, Via Opera Pia 11A, 16145 Genova, Italy

² ASTM Sagl, Via Comacini 7, 6830 Chiasso, Switzerland

ABSTRACT

One of our previous studies, published in the ACTA IMEKO journal, pointed out the probable variability in track-to-ground conductance measurements due to the use of the method indicated in A.3 of the international standard IEC 62128-2. In this work, the presence of measurement variabilities due to the connection of the negative terminal of the power supply to an earthing electrode instead of the behind section and due to the location chosen for the voltage terminal was proven by on-site measurements. A simulation model that includes undesirable soil conditions is proposed and used herein in the estimation of the correct value of track-to-ground conductance

Keywords: Conductivity measurement; DC power systems; electric variables measurement; grounding; guideway transportation power systems; guideway transportation testing; stray current

Citation: Jacopo Bongiorno, Andrea Mariscotti, Variability of measured railway track conductance due to test setup, Acta IMEKO, vol. 7, no. 4, article 5, December 2018, identifier: IMEKO-ACTA-07 (2018)-04-05

Editor: Alexandru Salceanu, "Gheorghe Asachi" Technical University of Iasi, Romania

Received March 28, 2018; **In final form** September 26, 2018; **Published** December 2018

Copyright: © 2018 IMEKO. This is an open-access article distributed under the terms of the Creative Commons Attribution 3.0 License, which permits unrestricted use, distribution, and reproduction in any medium, provided the original author and source are credited

Corresponding author: Jacopo Bongiorno, jacopo.bongiorno@edu.unige.it

1. INTRODUCTION

The stray current phenomenon, particularly significant for DC electrified transportation systems, is directly related to the insulation level of the traction current return path from surrounding structures and soil [1][2]. A known effect of stray current is the initiated and/or accelerated corrosion on metallic structures and on the rails themselves. This process is more evident and serious for larger leaking traction return currents [3]-[5]. A correct measurement of rail-to-earth conductance is therefore crucial during the entire life of an electrified transportation system.

The IEC 62128-2 international standard [6] identifies some measurement methods for track-to-ground conductance, which, however, are affected by profound variability due not only to the characteristics of the measured system, but also to the applied method itself. In a previous work, measurement variability introduced by various parameters was numerically evaluated [7] and estimated as lower than 1%. Rail-to-earth conductance values, however, depend on several factors, which can hardly be thoroughly modeled or accurately predicted [8]. Therefore, confirmation of the results using on-site measurements is necessary.

Variability due to the location of the voltage terminal by performing track-to-earth measurement following A.3. of IEC 62128-2 is thus experimentally assessed herein. The simulation

model used in [7] and [9] is improved by including a simple soil model.

As is commonplace, when performing measurements during the installation phases of a system [10], the installed tracks behind the measured section, which IEC 62128-2 identifies as the grounding path for the negative terminal of the power supply, may be unavailable. This negative terminal must be connected to grounded structures or to an electrode driven into the soil. Consequently, the resistance to ground of the power supply's negative circuit may take highly different values, which has an impact on the measured track insulation [7].

IEC 62128-2 [6] does not impose a unique location that is related to section length where the voltage reading is needed for the measurement. The choice of location introduces variability in track-to-ground conductance measurement results. This variability has been estimated in a simulation as being lower than 1% of the measured value.

In this work, the abovementioned variabilities are demonstrated and quantified using on-site measurements and are compared with the estimate obtained by the simulation.

2. THE TRACK-TO-GROUND CONDUCTANCE MEASUREMENT METHOD REPORTED IN IEC 62128-2

IEC 62128-2 [6] proposes and describes in its Appendix A, section A.3, a track conductance measurement method, shown in the schematic in Figure 1. Its use is suggested in the case of a

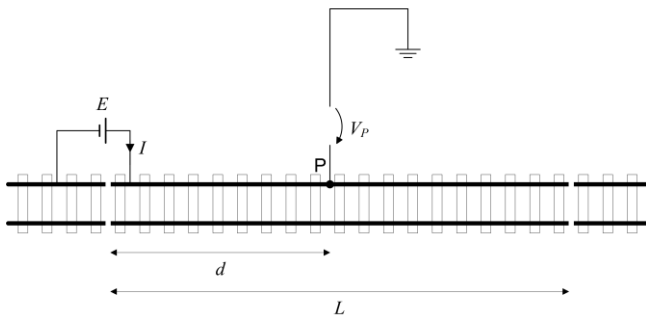


Figure 1. Test setup for track conductance (IEC 62128-2 Annex A.3).

track section that is delimited by an electrical separation of running rails, e.g., by rail cuts or insulated rail joints (IRJs). The section length L must be less than 2 km.

A DC voltage power supply (PS) is connected across the first rail cut and is used to obtain a nearly constant current, which flows from the measured track to the earth. The higher the track-to-earth conductance within the measured section, the larger the current that leaks from track to earth. In this paper, we identify with the term “measured section” or “track section” either the track or single rail, if there is no need to specify the real configuration.

The PS current I and voltage to ground V_p at a distance d from the current injection point are the measured quantities. The V_p voltage is measured against a reference electrode (RE) or a grounding circuit that is used as reference concerning which track conductance is quantified (e.g., concrete reinforcement, stray current collector, stray current mesh). The standard considers the ground reference as ideal and gives precise indications about its distance from the track, which, however, cannot be always fulfilled in real situations and are applicable to point electrodes, not distributed circuits. IEC 62128-2 does not require a specific distance d to use for the V_p measurement or the characteristics of the track behind section to which the negative terminal of the power supply should be connected.

The conductance to earth is estimated as:

$$G = \frac{I}{V_p L} \quad (1)$$

3. SIMULATION MODEL

The model used for theoretical calculations that was originally proposed and used in [7] and [9] is improved herein in terms of its representation of the return path resistance (the parallel connection of various conductive parts, unideal soil, and concrete). The improved model is implemented using Matlab Simulink. The equivalent circuit is shown in Figure 2.

The Simulink model is solved by using the ode15 method for ordinary differential equation systems.

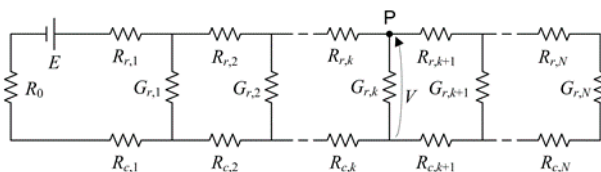


Figure 2. Equivalent circuit of the measured track section. Voltage source E is applied with a positive pole on the track and a negative pole on the “grounding electrode (GE)”/“behind section.” The potential V is measured at the volt-metric point P .

4. VARIABILITY OF RESULTS

In this section, variabilities due to the earthing resistance of the PS negative terminal (R_0), the change in location of the volt-metric measurement point P , and the effect of the different resistance levels of the return path (e.g. for different soil types) are analyzed and experimentally verified. As pointed out in Section 1 and in [7], there are many sources of variability in rail-to-earth conductance measurements using the method of IEC 62128-2. Some variabilities can be avoided by taking precautions when performing measurements, but others depend on contingency, site characteristics, the availability of connections, etc.

4.1. Description of the measured sections

Measurements from four different sites are considered herein, named A through D. Two sites were used to verify the influence of the resistance to earth of the PS negative terminal (sections A and B). The results for two other sites are reported (sections C and D) to support the assessment of variability of track-to-earth conductance for different positions of the volt-metric probe P .

Section lengths for short sections are rounded to the first decimal place, with ± 5 cm accuracy that is better than 1 %. When the length is longer than 100 m, the rounding is to 1 m, again with accuracy that is better than 1 %. The measured resistance values are expressed with ≤ 0.5 % precision compared to a combined uncertainty of the voltage and current measurements with accuracy that is better than 1 % (with coverage factor $k=2$). Estimated values, characterized by a larger and inaccurately quantified uncertainty due to the many quantities and conditions involved, are always rounded to the nearest integer. The calculated conductance-to-earth values are expressed in S/km with a precision of three decimal places (about 0.1 %). The estimated variability of conductance-to-earth values has similar precision.

The length of section A is 74.9 m, and the measured rail p.u.l. resistance is 43.15 m Ω /km. Section A is characterized by a very short section of behind tracks connected to the negative terminal of the PS, and the resistance to ground of this section is estimated in 93 Ω . As the resistance to ground of the PS negative terminal connected to the behind tracks is high, one copper electrode driven into the soil was used as alternative grounding, with a resistance to ground of about 60 Ω (see section 4.2.1). The length of section B is 60.8 m, and the measured rail p.u.l. resistance is 42.27 m Ω /km. This section, unlike the other section A, has a very long track section behind it, with an estimated resistance to ground of lower than 5 Ω (see section 4.2.1). For both sections A and B, a copper electrode was driven into the soil to be used as alternative grounding means for the PS and its resistance to earth was measured (see section 4.2.1).

Section C is a tunnel section of 1917 m. It is very well insulated and was measured using the stray current collector as a reference. The measurement current flows from the rails into the slab beneath them and then returns to the negative terminal of the PS using the preferential low resistance method represented by the stray current mesh and the stray current collector. In this case, the measurement current return path resistance has the order of magnitude specified by 0.07 Ω /km, estimated based on the premise that the longitudinal stray current mesh and collector are electrically in parallel.

Section D is a cut-and-cover section of 454 m, measured using copper sulfate electrodes positioned on an almost dry concrete wall (surfaces at the electrode-concrete interface were

Table 1. Rail-to-ground conductance measurement and variations against different resistance to ground of the power supply.

Site	R_0 in Ω	G_{meas} in S/km	ΔG_{meas}	G_{sim} in S/km	ΔG_{sim}
A1	92.9	0.380	$\pm 1.6\%$	0.374	$< \pm 0.1\%$
	59.0	0.368		0.374	
A2	92.9	1.299	$\pm 8.0\%$	1.204	$\pm 0.1\%$
	59.0	1.107		1.204	
B1	5	2.639	$\pm 0.6\%$	2.657	$< \pm 0.1\%$
	61.4	2.672		2.628	
B2	5	2.516	$\pm 1.0\%$	2.543	$< \pm 0.1\%$
	61.4	2.569		2.545	

kept humid by pouring water on them). In this case, the return path resistance is higher, estimated in the range of 10-1000 Ω /km, using Table 7 of [11]. It worth stressing that this section was purposely chosen to emphasize the effect of different P locations and to demonstrate the effect of poor conductive soil or material used as return conductor.

4.2. Measurements

The site measurements of the rail-to-earth conductance were performed with the aims of demonstrating the variability due to the PS earthing resistance and of validating the numerical models used. The measurements of rail-to-earth conductance for sections A to D are considered. The preliminary steps were the measurement of the resistance to ground of the PS grounding electrode (GE) and the estimation of the resistance to earth of the track section behind.

4.2.1. Influence of grounding electrode (GE) resistance

The used GE is a copper cylindrical rod with a length of 1.50 m and a diameter of 2.54 cm.

The GE resistance to ground was measured using an AEMC/Chauvin Arnoux mod. 6471 “digital ground resistance and soil resistivity tester” [12]. The method used is the three-pole earth/ground measurement with the 62 % rule [13]. Two auxiliary electrodes (EH and ES) were placed in a straight line from the electrode being tested, complying with the 62 % rule. The electrode S, the closest to the measured electrode GE, was placed at a distance $d=10.50$ m, more than eight times the driven depth of the GE (1.10 m). The electrode EH was placed in a straight line with electrodes GE and ES at a distance $d=62\%$. The measurement was repeated, rotating the electrodes EH and ES in three different positions around the electrode GE for verifying the homogeneity of the surrounding soil and the absence of interference from external sources.

The track-to-earth resistance of the track section behind the injection point was estimated using, as input values, the track length and an estimated conductance value of 0.092 S/km, in agreement with the values obtained from conductance measurements performed on other similar tracks and assuming the homogeneous behavior of the insulation.

Site A. The measured value of the GE earthing resistance is 59.0 Ω , with an instrument error declared by AEMC of $\pm 2\%$. The spread of the three measured soil resistivity values around the GE is $\pm 1.5\%$ of the mean. The low variability indicates a good homogeneity of the soil as well as low instrument uncertainty. The track section behind the injection points in this site was very short, 117 m, leading to an estimated resistance to earth of 92.9 Ω .

Site B. The measured value of the GE earthing resistance is 61.4 Ω , with an intrinsic error declared by the manufacturer (AEMC) of $\pm 2\%$. The spread among the three measured soil resistivity values is $\pm 1.7\%$ of the mean. The low variability again indicates good soil homogeneity and low instrument uncertainty.

The track section behind the injection point was very long in this site, more than 2 km. As the precise length could not be measured, a value of 5 Ω is assumed for its resistance to ground.

The results of the rail-to-ground conductance measurements for both sites A and B are shown in Table 1. The volt-metric measurement point P is fixed at 60 m from the injection point, and the reference electrode (RE) is placed 30 m away from the track axis. The column “ ΔG_{meas} ” represents the spread in % around the calculated mean. The values of the resistance to earth of the PS negative pole are shown in column “ R_0 .”

The measured conductance variability, depending on R_0 , is clearly visible for all measurements. The measured rail-to-ground conductance increases for larger R_0 values. The observed spread around the mean value is about $\pm 1-2\%$ with a peak value of $\pm 8.0\%$ for the measurement A2, where, however, the RE for the volt-metric measurement at point P was placed at the opposite side of the measured rail. In a different way, for all other measurements, the reference electrodes were placed always at the same side of the track of the measured rail. The presence of the other rail in the path between the measured rail and the reference electrode can disturb the electric field created by the measured rail, and the measurements are affected by this distortion.

4.2.2. Track-to-ground conductance value vs. potential measurement point P

Measurements at sections C and D were performed, moving P along the track, with a PS earthing resistance of $< 3 \Omega$.

Site C. The first P point was located at 63.0 m from the injection point and the other three locations were chosen at 177 m, 487 m, 1126 m from the injection point. The PS current return path resistance is calculated as 0.07 Ω /km, as anticipated in section 4.1. The measured section track-to-earth conductance values were very low, giving 0.00132 $\pm 1.5\%$ S/km. The variability is thus comparable with the instrumental uncertainty, and it is difficult to link it back to P moving between locations. The measurement is, however, used as a check for consistency in the simulation results because, for these values of conductance and return path resistance, the simulated variability should not be larger than the measured one.

Site D. Site D is more interesting. The measurement was performed with a specific return path through concrete. P was moved in four 35 m steps from 135 to 310 m from the PS injection point. The measurement results, together with the error bars that represent the $\pm 5\%$ measurement variability, are shown in Figure 3 for the five different P locations. The results take into account the single measurement point and the least-square fit of the data in order to compensate for the random errors in the measurements. The measurement was repeated later in the same section D using method A.2 of IEC 62128-2 in order to confirm the order of magnitude of the results obtained using the first measurement. The track-to-earth conductance using method A.2 and similar environmental conditions was 0.206 S/km $\pm 5\%$.

4.3. Simulation

As mentioned in the previous section, the numerical calculation performed in [7] shows that the variability of the measured conductance due to the test setup highly depends on

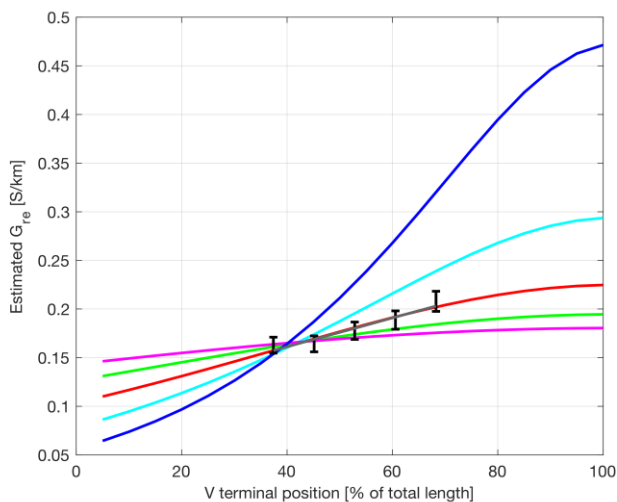


Figure 3. Rail-to-earth conductance for site D by moving V terminal position: measured values (error bars $\pm 5\%$ of measured value) and least-square interpolation (line).

the physical characteristics of the measured system (e.g., real conductance, soil characteristics, and track length). New numerical calculations using an improved Simulink model (which includes a soil model) were performed in order to obtain the results of theoretical variability to compare with the measurements for sites A through D. The input parameters of the model are therefore set according to the physical parameters of the system discussed so far.

The results of the numerical calculations for the R_0 effect are shown in Table 1, where the column " ΔG_{sim} " represents the variability of the simulated values in percentage, considering the two different values of R_0 when using the track section behind and a vertical GE. The simulated variability of the resulting conductance is always lower than $\pm 0.03\%$ around the mean of the two calculated results.

The simulation results for site C, varying the location of the volt-metric point P, show a variability lower than $\pm 0.0001\%$, with a simulated conductance of 0.00132 S/km . The whole dataset is not reported here in the form of a figure or table since, due to the very low variability, it is considered insignificant.

The simulation results for site D considering variability due to the volt-metric point P are shown in Figure 4. As the value assigned to the concrete resistivity is an estimation based on typical values identified in Table 7 of [11], but no measurements were performed to assess this point, a sensitivity analysis is reported in Figure 4, considering $220\ \Omega/\text{km}$, $110\ \Omega/\text{km}$, $55\ \Omega/\text{km}$, $22.75\ \Omega/\text{km}$, and $13.75\ \Omega/\text{km}$, using as input track-to-earth conductance value of 0.167 S/km .

4.4. Comparison

The measurement results reported in Table 1 show that for both sites A and B, the simulated variability of the track-to-earth conductance due to R_0 highly underestimates the variability that occurs in real measurements. The underestimation is about two orders of magnitude, and for measurement A2, it increases to three orders of magnitude.

When the first simulations with the lumped circuit simplified were done, it was thought that the extreme simplicity of the model, neglecting soil resistivity, discontinuities, field distortion due to conductors in the nearby area, etc., would have justified such difference. However, using the improved model that

includes the resistivity of the current return path through structure and soil, the simulation results have not changed. The observed variability thus reflects that different positions of the negative terminal of the PS imply different current distributions in the soil, intercepting different layers at different depths with variable resistivity.

The simulation results for site C, varying the location of the volt-metric point P, are comparable with the measured results. Setting in the model a track-to-earth conductance value that is equal to the one measured, 0.00132 S/km , the simulated variability is lower than $\pm 0.0001\%$ and is thus insignificant because the measurement variability of such measurement has the order of magnitude specified by $\pm 1\%$ of the measured value (see section 4.2.2). The whole dataset is not reported here in the form of a figure or table, as it is considered insignificant.

Figure 4 shows that the simulation results, varying the volt-metric point P, are in accordance with the measurement results for site D, using an estimated resistivity of the measurement current return path of $55\ \Omega/\text{km}$. After having determined the simulated curve, which shows very good similarity between the simulation results and the measurement least-square interpolation, estimation of the real track-to-ground conductance is possible, considering the input value of the simulation, 0.167 S/km , as real. This conductance is comparable with that measured using the A.2 method, as detailed in section 4.2.2.

5. CONCLUSION

The variability in rail-to-earth conductance measurements due to different resistance to ground levels in the PS and the different locations of the volt-metric terminal used to apply the methods described in A.3 of IEC 62218-2 [6] has been experimentally verified. A comparison with numerical simulations concerning the variability due to the resistance of the negative terminal of the PS has shown that, in real cases, the variability is larger than numerical calculations predict. It was anticipated that an improved model that includes the soil resistivity of the measurement current return path would have improved the

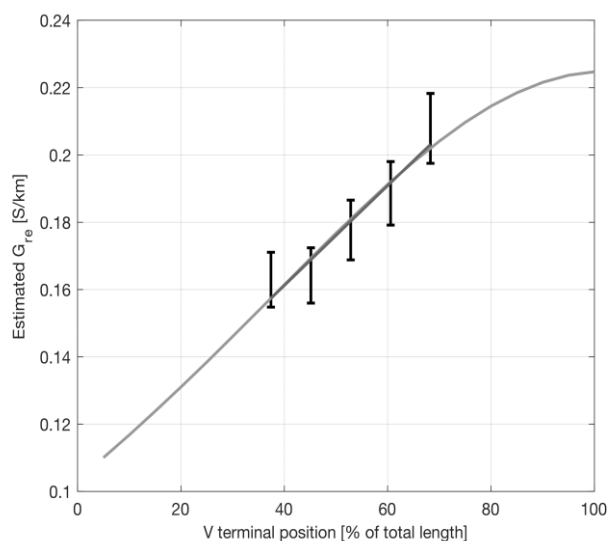


Figure 4. Comparison of rail-to-earth conductance values of site D: measured (error bars $\pm 5\%$ of measured value), measured with least-square interpolation (black line), and predicted (curves for concrete resistivity values of $220\ \Omega/\text{km}$ [blue], $110\ \Omega/\text{km}$ [light blue], $55\ \Omega/\text{km}$ [red], $27.5\ \Omega/\text{km}$ [green], $13.75\ \Omega/\text{km}$ [magenta]).

similarity between the measured and simulated data, but the expected improvement was not obtained. The observed variability thus reflects that the different positions of the negative terminal of the PS imply different current distributions in the soil, intercepting different layers at different depths, with variable resistivity. Our advice is that, in case the earthing electrode for the negative terminal of the PS is used instead of the behind section of the track, two checks should be performed: the resistance to earth of the electrode should be much lower than the measured track-to-ground resistance, and the absence of highly resistive soil zones near the track should be ascertained. The variability in rail-to-earth conductance measurements due to the grounding resistance of the PS in real cases is about a few percent but increases up to about 10 % when the reference electrode for the volt-metric measurement is placed opposite the measured rail. This behavior indicates that the volt-metric reference electrode should be placed on the same side of the measured rail.

In other cases, a variability of some percent of measured conductance results can, however, be considered acceptable for the type of measurement.

Variability that occurs due to different volt-metric point (P) locations along the measured track section is generally irrelevant, since it is lower than the variability that is due to random measurement errors. However, it was seen to have increased in the case of high resistance of the measurement current return path (through concrete instead of soil in the measured scenario). A correction factor based on the proposed model might be proposed to find the correct track-to-earth conductance value in the unideal case of low current return path resistance. Future researchers could analyze the behavior of the simulated results (that are now validated) by changing the relevant parameters (the resistivity of the measured current return path, rail resistivity, or the track-to-earth conductance itself) in order to extrapolate some general rules about conditions in which variability due to test setup becomes relevant.

6. REFERENCES

- [1] P. Aylott, The application of modelling systems at the design stage to the mitigation of stray current interference, Corrosion 2003, NACE International.
- [2] A. Ogunsola, A. Mariscotti, L. Sandrolini, Estimation of stray current from a DC-electrified railway and impressed potential on a buried pipe, IEEE Transaction on Power Delivery 27(4) (2012) pp. 2238-2246.
- [3] T. Barlo, A. Zudnek, Stray Current Corrosion in Electrified Rail Systems, Final Report, Northwest Engineering Publications, May 1995.
- [4] L. Bertolini, M. Carsana, P. Pedefferri, Corrosion behaviour of steel in concrete in the presence of stray current, Corrosion Science 49(3) (2007) pp. 1056-1068.
- [5] A. Ogunsola, L. Sandrolini, A. Mariscotti, Evaluation of stray current from a DC-electrified railway with integrated electric-electromechanical modeling and traffic simulation, IEEE Transactions on Industry Applications 51(6) (2015) pp. 5431-5441.
- [6] IEC 62128-2, Railway applications - Fixed installations - Electrical safety, earthing and the return circuit - Part 2: Provisions against the effects of stray currents caused by d.c. traction systems, 2012.
- [7] J. Bongiorno, A. Mariscotti, Accuracy of railway track conductance and joint efficiency measurement methods, Acta IMEKO, 4(4) (2015) pp. 82-87.
- [8] C. Charalambous, I. Cotton, P. Aylott, A simulation tool to predict the impact of soil topologies on coupling between a light rail system and buried third-party infrastructure, IEEE Transactions on Vehicular Technology 57(3) (2008) pp. 1404-1416.
- [9] J. Bongiorno, A. Mariscotti, Variability of track-to-ground conductance measurement, Proc. of 22nd IMEKO TC4 Symposium, pp. 106-110, Sept. 14-15, 2017, Iasi, Romania.
- [10] P. Aylott, I. Cotton, C. Charalambous, Impact and management of stray current on DC rail systems, IET Seminar Digest, 2011.
- [11] IEEE Std 80, IEEE Guide for Safety in AC Substation Grounding, Feb. 2013.
- [12] AEMC/Chauvin Arnoux, Digital ground resistance and soil resistivity tester mod. 6471 (User Manual).
- [13] F. Dawalibi, C. Mukhledkar, Ground electrode resistance measurements in non-uniform soils, Power Apparatus and Systems (1973) pp. 109-115.